PCP
PLANT & CELL PHYSIOLOGY

A DEAD-Box Protein, AtRH36, is Essential for Female Gametophyte Development and is Involved in rRNA Biogenesis in Arabidopsis

Chun-Kai Huang[1], Li-Fen Huang[2], Jin-Ji Huang[1], Shaw-Jye Wu[1], Ching-Hui Yeh[1] and Chung-An Lu[1,*]

[1]Department of Life Science, National Central University, Jhongli City, Taoyuan County 320, Taiwan, ROC
[2]Graduate School of Biotechnology and Bioengineering, Yuan Ze University, Jhongli City, Taoyuan County 320, Taiwan 320, ROC
*Corresponding author: E-mail, chungan@cc.ncu.edu.tw; Fax, +886-3-4228482
(Received January 27, 2010; Accepted April 4, 2010)

Regular Paper

DEAD-box RNA helicases are involved in RNA metabolism, including pre-mRNA splicing, ribosome biogenesis, RNA decay and gene expression. In this study, we identified a homolog of the *RH36* gene, *AtRH36*, which encodes a DEAD-box protein in *Arabidopsis thaliana*. The gene was expressed ubiquitously throughout the plant. The AtRH36 fused to green fluorescent protein was localized in the nucleus. Homozygosity for the Arabidopsis *atrh36* mutants, *atrh36-1* and *atrh36-2*, could not be obtained. Progeny of selfed Arabidopsis *atrh36* heterozygote plants were obtained at a heterozygote to wild-type ratio of 1 : 1, which suggested that the *AtRH36* gene was involved in gametogenesis. Therefore, we performed a reciprocal cross to determine whether *AtRH36* was involved in female gametophyte development. Female gametogenesis was delayed in *atrh36-1*, and asynchronous development of the female gametophytes was found within a single pistil. Knock-down of *AtRH36* gave a pleiotropic phenotype and led to the accumulation of unprocessed 18S pre-rRNA. These results suggest that AtRH36 is essential for mitotic division during female gametogenesis and plays an important role in rRNA biogenesis in Arabidopsis.

Keywords: *Arabidopsis thaliana* • DEAD-box helicase • Female gametogenesis • rRNA biogenesis.

Abbreviations: CLSM, confocal laser scanning microscopy; DMSO, dimethylsulfoxide; ETS, external transcribed spacer; GFP, green fluorescent protein; GUS, β-glucuronidase; ITS, internal transcribed spacer; MS, Murashige and Skoog; RNAi, RNA interference; RT–PCR, reverse transcription–PCR; SF2, superfamily 2.

Introduction

RNA molecules have multiple functions, for example they carry genetic information and have catalytic activities. RNA is synthesized and processed in the nucleus and then transported to the cytoplasm. Depending on the specific functions of the RNA molecules, they can form a long single strand or a compact molecule folded into a complex tertiary structure. DEAD-box proteins ensure that RNA molecules are folded correctly by maintaining or modifying specific secondary or tertiary RNA structures (de la Cruz et al. 1999). DEAD-box proteins are classified as members of the helicase superfamily 2 (SF2) on the basis of amino acid sequence homology within the helicase domain. SF2 contains three subfamilies, DEAD, DEAH and DExH/D, based on variations in amino acid sequence within motif II of the proteins (de la Cruz et al. 1999, Tanner and Linder 2001, Linder and Owttrim 2009). The DEAD-box family is the largest family of RNA helicases, and contains the amino acid sequence Asp-Glu-Ala-Asp (D-E-A-D) in motif II. DEAD-box proteins are referred to as energy-dependent RNA helicases that unwind the double-stranded RNA (dsRNA). However, the unwinding activity of DEAD-box proteins is limited to short duplexes of dsRNA; hence, only local dissociation of dsRNA occurs (Linder 2006, Linder and Lasko 2006, Sengoku et al. 2006, Pyle 2008). In addition, DEAD-box proteins can rearrange ribonucleoprotein (RNP) complexes via direct dissociation of RNA–protein complexes or modification of RNA structures (Chen et al. 2001, Kistler and Guthrie 2001, Linder 2006, Pyle et al. 2007, Pyle 2008).

DEAD-box proteins are found in all eukaryotes and most prokaryotes (Aubourg et al. 1999, de la Cruz et al. 1999, Rocak and Linder 2004). In yeast, 25 DEAD-box proteins have been identified (de la Cruz et al. 1999, Linder et al. 2000). Through biochemical and genetic approaches, DEAD-box proteins have been shown to be involved in almost all processes of RNA metabolism, including nuclear transcription, pre-mRNA splicing, ribosome biogenesis, nucleo-cytoplasmic transport, translation, decay, and gene expression in organelles (Rocak and Linder 2004, Cordin et al. 2006). Despite the amino acid sequence homology of DEAD-box proteins within the core

Plant Cell Physiol. 51(5): 694–706 (2010) doi:10.1093/pcp/pcq045, available online at www.pcp.oxfordjournals.org

helicase regions, each DEAD-box protein seems to have a specific biological function within the cell. For example, 14 different DEAD-box proteins are required for ribosome biogenesis in yeast, and the absence of any one of these genes leads to a lethal phenotype (Cordin et al. 2006, Linder 2006). Although it has been proposed that DEAD-box proteins are involved in several different cellular processes, their actual roles remain to be further elucidated.

DEAD-box proteins constitute a large gene family in plants. There are at least 58 DEAD-box proteins in Arabidopsis (*Arabidopsis thaliana*) (Aubourg et al. 1999, Boudet et al. 2001). Several studies have suggested that the DEAD-box proteins play important roles in plant growth and development and in responses to biotic and abiotic stresses (Okanami et al. 1998, Jacobsen et al. 1999, Wang et al. 2000, Li et al. 2001, Park et al. 2002, Gendra et al. 2004, Gong et al. 2005, Matthes et al. 2007, Shimizu et al. 2008, Linder and Owttrim 2009, Stonebloom et al. 2009). For example, the Arabidopsis DEAD-box protein LOS4 is essential for mRNA export and important for stress responses and development (Gong et al. 2005). The protein MAGATAMA3 is an Arabidopsis homolog of the yeast DEAD-box protein Sen1, which functions in the maturation of tRNA, small nuclear RNA, rRNA and mRNA (Winey and Culbertson 1988). MAGATAMA3 is required for the development of female gametophytes and guidance of the pollen tube (Shimizu et al. 2008). Arabidopsis CARPEL FACTORY/DICER-LIKE 1, a DExH/DEAD-box RNA helicase, appears to suppress cell division in floral meristems (Jacobsen et al. 1999). ISE1, an Arabidopsis DEAD-box protein, localizes to mitochondria and is essential for mitochondrial function in regulating cell–cell transport via plasmodesmata. Loss of ISE1 leads to an embryo-lethal phenotype in Arabidopsis (Stonebloom et al. 2009). The tobacco VDL gene, which encodes a plastid DEAD-box protein, is involved in chloroplast differentiation and plant morphogenesis (Wang et al. 2000). Three DEAD-box proteins, AtRH5 (At1g31970), AtRH9 (At5g60990) and AtRH25 (At5g08620), are involved in responses to multiple abiotic stresses in Arabidopsis (Kant et al. 2007, Kim et al. 2008). OsBIRH1, which is a rice DEAD-box protein, modulates defense responses to pathogen infection and oxidative stress (Li et al. 2008). However, the biological functions of most plant DEAD-box proteins are not clear and require further study.

In the study reported herein, we investigated the biological role of the DEAD-box protein AtRH36, a homolog of yeast Dbp8p, in plants. Characterization of the *AtRH36* gene in Arabidopsis and genetic complementation suggested that *AtRH36* is essential for the development of female gametophytes and is required for the normal progression of mitotic division cycles during gametogenesis. Knock-down of *AtRH36* expression resulted in several morphological phenotypes, which indicates that AtRH36 is involved in multiple developmental pathways. Furthermore, we showed that AtRH36 plays a role in rRNA biogenesis in Arabidopsis.

Results

RH36 encodes a DEAD-box RNA helicase

To study the role of RH36 in plants, a cDNA fragment of *AtRH36* was isolated, and found to encode a protein of 491 amino acids with nine conserved RNA helicase motifs and two nuclear localization signals at its C-terminus. The phylogenetic tree of RH36 proteins showed that AtRH36 and OsRH36 were grouped together and were closely related to yeast Dbp8p and human DDX49 (**Fig. 1A**). The degree of amino acid sequence identity between AtRH36 and OsRH36 was 57%. AtRH36 shared 45% identity and 63% similarity with yeast Dbp8p. With respect to human DDX49, AtRH36 shared 48% identity and 69% similarity.

Subcellular localization and expression pattern of AtRH36

To determine the subcellular localization of AtRH36, we generated a construct that encoded AtRH36–green fluorescent protein (GFP) under the control of a *35S* promoter and introduced the construct into onion epidermal cells by particle bombardment. In cells transformed with *35S* promoter::*AtRH36–GFP*, the GFP fluorescence signal was only detected in the nucleus, with dense spots which were co-localized with the nucleolus (**Fig. 1B–E**). In contrast, in cells transformed with *35S* promoter::*GFP*, the GFP fluorescence signal was detected in the nucleus and the cytoplasm (**Fig. 1F, G**). These results indicated that AtRH36–GFP fusion protein localized to the nucleus and nucleolus.

To determine the expression pattern of the *AtRH36* gene in Arabidopsis, reverse transcription–PCR (RT–PCR) was performed. Total RNA was isolated from a variety of tissues, and specific primers were used to detect *AtRH36* and *Actin* (*Act1*, *At2g37620*) mRNA. **Fig. 1H** shows that *AtRH36* mRNA was present in all of the organs selected, including rosette leaves, cauline leaves, stems, roots, flowers and siliques. These results indicated that *AtRH36* was expressed ubiquitously throughout the plant. On the other hand, expression of *AtRH36* is induced by glucose from microarray data that are available at the GENEVESTIGATOR database (https://www.genevestigator.ethz.ch) (**Fig. 1I**).

The promoter activity of the *AtRH36* genes was analyzed further by using a β-glucuronidase (GUS) reporter. The *AtRH36* promoter (469 bp) was fused upstream of the GUS reporter gene *uidA* and expressed in Arabidopsis. More than 30 independent transgenic plants were obtained for the expression construct. Three transformants that carried transgenes were selected for further analysis of GUS expression. T_2 transgenic Arabidopsis lines that contained the *uidA* gene driven by the *AtRH36* promoter showed GUS expression in most vegetative organs, including roots, cotyledons, leaves, trichomes and inflorescence stems (**Fig. 1J–L**). GUS activity was also detected in reproductive organs, such as stigmata, anthers, petals and

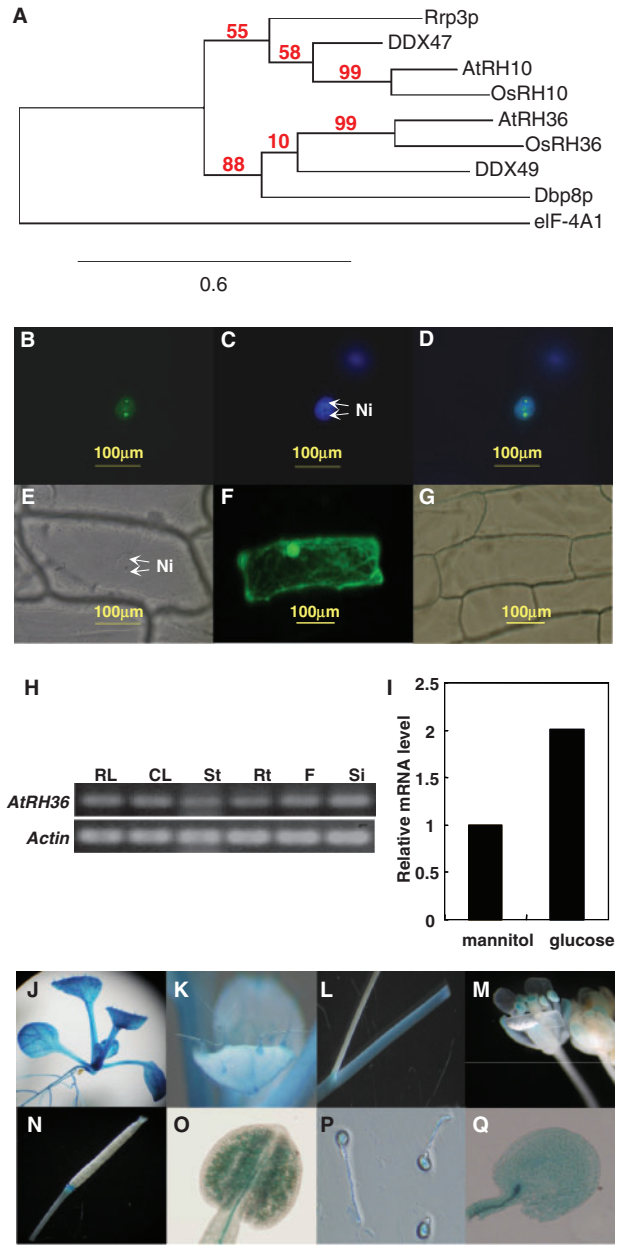

Fig. 1 Subcellular localization and expression of AtRH36. (A) A phylogenetic tree of RH36 proteins generated by TCofee and PhylML. The following RNA helicases are shown: AtRH36 (*A. thaliana*, NM_101494), AtRH10 (*A. thaliana*, NP_568931), eIF-4A1 (*A. thaliana*, NP_566469), OsRH36 (*O. sativa*, NP_918000), OsRH10 (*O. sativa*, NP_001050861), Dbp8p (*Saccharomyces cerevisiae*, NP_012039), Rrp3p (*S. cerevisiae*, NP_011932), DDX49 (*Homo sapiens*, NP_061943.2) and DDX47 (*H. sapiens*, NP_057439.2). (B–G) Onion epidermal cells transformed with 35S promoter::*AtRH36–GFP* (B–E) or 35S promoter::*GFP* (F and G). (B and F) Images of green fluorescent fields; (C) an image of a DAPI (4′,6-diamidino-2-phenylindole) fluorescent field; (D) a composite image of green and DAPI fluorescence; (E and G) bright field images. Ni, nucleolus; Bars = 100 μm. (H) RT–PCR analysis of *AtRH36* gene expression in Arabidopsis. Total RNA was isolated from the rosette leaves (RL), cauline leaves (CL), stems (St), roots (Rt), flowers (F) and siliques (Si) of mature Arabidopsis plants. Arabidopsis *Actin* was used as an internal control. (I) Expression of *AtRH36* was induced by glucose. The *y*-axis represents the relative mRNA expression level, using mannitol treatment as 1. Gene expression patterns were obtained from the publicly available microarray data at GENEVESTIGATOR (https://www.genevestigator.ethz.ch). (J–Q) GUS activity in Arabidopsis transgenic lines that carried the *AtRH36* promoter fusion construct. GUS activity in seedling (J), trichomes (K), stems (L), flowers (M), silique (N), stamen (O), pollen grains and pollen tubes (P), and ovule (Q).

siliques (**Fig. 1M, N**). Moreover, close observation showed that expression of GUS could be detected in pollen grains, vascular tissues of the stamen, pollen tubes and ovules (**Fig. 1O–Q**). Therefore, GUS activity could be detected in most organs and tissues of the transgenic Arabidopsis plants, which indicated that the *AtRH36* gene was transcribed ubiquitously during different stages of plant development.

Mutations in AtRH36 exhibit distorted segregation

To elucidate the biological role of AtRH36 in Arabidopsis, three transfer DNA (T-DNA) insertion lines, *atrh36-1* (Salk_102486), *atrh36-2* (Salk_079348) and *atrh36-3* (Salk_045190), were identified and characterized (**Fig. 2A**). The genotypes of the progeny from self-crosses of the *atrh36* heterozygous mutants were analyzed by PCR-based screening. The results of this analysis revealed that all 249 analyzed progeny plants from either *atrh36-1* or *atrh36-2* heterozygous parents were heterozygous or wild type (**Fig. 2B, C**; **Table 1**). However, approximately 15% of the progeny from *atrh36-3* heterozygous plants were homozygous for the mutant allele (**Table 1**). The expression level of the *AtRH36* transcript in the *atrh36-3* homozygous plants was similar to that in the wild type, as shown by RT–PCR analysis (**Supplementary Fig. S1C**). Moreover, the *atrh36-3* homozygous plants did not show morphological differences compared with the wild type plants (**Supplementary Fig. S1D, E**). Therefore, in the *atrh36-3* mutant line, the T-DNA insertion in the promoter region did not affect the expression of the *AtRH36* gene, and this might explain why homozygotes were only obtained for the *atrh36-3* mutant allele. These results indicated that no homozygous *AtRH36* knock-out plant could be obtained among all examined progeny.

To confirm this conclusion, a binary vector that contained the genomic DNA for *AtRH36* fused to its own promoter and terminator was transformed into *atrh36-1* heterozygous plants for functional complementation (**Fig. 2D**). Three independent T_1 hygromycin-resistant transformants were selected, and the genotypes of the progeny plants were analyzed. The analysis indicated that *atrh36-1* homozygous plants were obtained in all selected T_2 progeny populations. One example is shown in **Fig. 2E**; four plants among eight randomly selected hygromycin-resistant T_2 plants did not contain the wild-type *AtRH36* allele (lines 3, 5, 6 and 7). The observation of homozygous *atrh36-1* alleles in transgenic plants indicated that the distorted

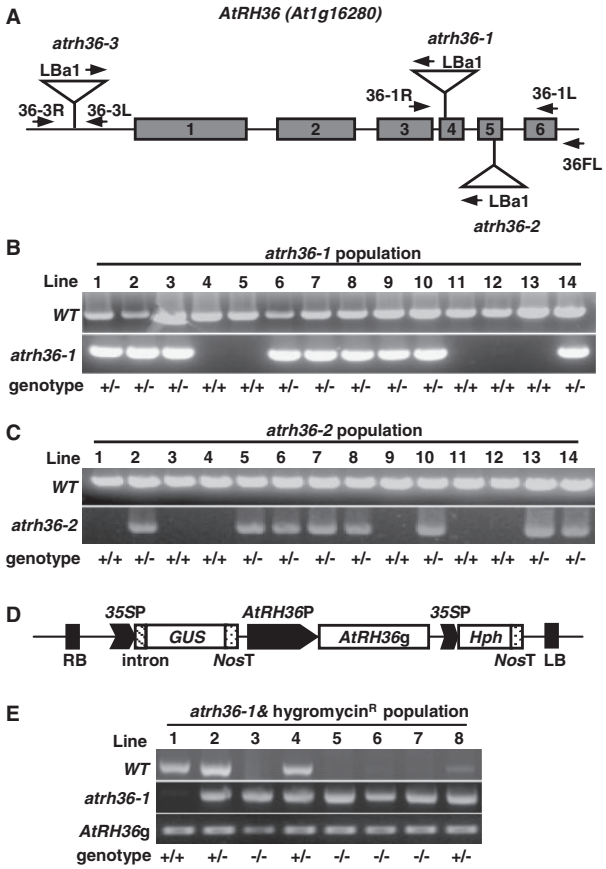

Fig. 2 Characterization of Arabidopsis *atrh36* mutants. (A) Structure of the *AtRH36* gene. Gray boxes represent exon sequences and lines represent non-coding sequences. The three T-DNA insertion alleles, *atrh36-1*, *atrh36-2* and *atrh36-3*, are indicated by open triangles. The positions of the primer sequences used for PCR genotyping of *AtRH36* (wild-type; WT) and the *atrh36* mutant alleles are marked with arrows. The primers 36-1R and 36-1L were used to screen the *atrh36-1* and *atrh36-2* mutants. The primers 36-3R and 36-3L were designed specifically for the *atrh36-3* mutant. The primers 36FL and 36-1R were designed to detect the endogenous *AtRH36* genomic sequence in the *atrh36-1* complementation test. (B and C) PCR-based genotype screening for *AtRH36* (*WT*) and the mutant alleles (*atrh36-1* in B and *atrh36-2* in C) in segregating populations derived from self-pollinated plants heterozygous for the *atrh36-1* (B) or *atrh36-2* (C) alleles. WT plants are indicated by +/+ and heterozygous mutant plants by +/−. (D) Schematic representation of the construct used for functional complementation. The vector contained the genomic DNA sequence of *AtRH36* (*AtRH36*g), its native promoter (*AtRH36*P) and terminator. In this vector, β-glucuronidase (*GUS*) containing one intron and the hygromycin resistance gene (*Hph*) were both under the control of the *CaMV35S* promoter (35SP) and the nopaline synthase terminator (*Nos*T). LB, left border; RB, right border. (E) The genotype of hygromycin-resistant T_2 transgenic plants that expressed *AtRH36* [obtained by using the binary vector shown in (D) to transform *atrh36-1* heterozygous plants] was identified by PCR. The primers 36-1R and 36FL were used to amplify specifically the *WT* allele, but not the transgene *AtRH36*g. The WT allele is indicated by + and the *atrh36-1* mutant allele by −.

Table 1 The genotype of progeny from self-crossed *atrh36* heterozygote mutant plants

Parent genotype	No. of progeny			Heterozygote/ wild type ratio
	+/+	+/m	m/m	
atrh36-1/AtRH36	82	70	0	0.85
atrh36-2/AtRH36	53	44	0	0.83
atrh36-3/AtRH36	6	10	3	1.67

+, represents wild-type allele; m, represents the mutant allele.

segregation could be fully complemented by expression of the *AtRH36* cDNA.

AtRH36 is involved in female gametophyte development

The wild type to heterozygote ratio of the progeny of the *atrh36-1* and *atrh36-2* heterozygotes was approximately 1:1 in Arabidopsis (**Table 1**); therefore, we hypothesized that AtRH36 might play an essential role in either gametophyte development or fertilization during plant reproduction. To determine whether the distortion in segregation was caused by a developmental defect during gametogenesis, we performed reciprocal crosses between the *atrh36-1* heterozygote and wild-type plants, and then counted each genotype among the progeny populations. As shown in **Table 2**, the F_1 progeny population from self-crossed *atrh36-1* heterozygous plants segregated with a 1:0.83 (53:44) ratio of wild-type to heterozygous plants. No transmission of the *atrh36-1* allele was observed when the *atrh36-1* heterozygote was used as the female parent and backcrossed with the wild type (*atrh36-1/AtRH36-1*×*AtRH36-1/AtRH36-1* in **Table 2**). On the other hand, when the *atrh36-1* heterozygote was used as the male parent and backcrossed with the wild type, the F_1 progeny population segregated in a 1:0.79 (181:143) ratio of wild-type to heterozygous plants (*AtRH36-1/AtRH36-1*×*atrh36-1/AtRH36-1* in **Table 2**). This showed that the transmission rate of the *atrh36-1* mutant allele was reduced only slightly compared with that of the wild-type allele. Therefore, we concluded that the *atrh36-1* allele could be transmitted through the male but not the female gametophyte.

The roots, leaves, shoots and flowers of *atrh36-1* heterozygous plants could not be distinguished morphologically from those of wild-type plants. However, *atrh36-1* heterozygous plants produced short siliques (**Fig. 3A, B**) and had a significant number of aborted seeds (**Fig. 3C, D**). The length of the siliques from *atrh36-1* heterozygotes was approximately two-thirds shorter than that of wild-type plants at the same age (**Fig. 3B**). Siliques were collected from self-crossed *atrh36-1* heterozygotes and the numbers of mature and aborted seeds were counted. The analyzed siliques from the *atrh36-1* heterozygous progeny contained 53% ($n = 655$) mature seeds and 47% ($n = 581$) aborted seeds, compared with 94.5% ($n = 565$) mature seeds and 5.5% ($n = 33$) aborted seeds in the wild-type progeny (**Fig. 3D**).

Table 2 Transmission efficiency of *atrh36-1* alleles

Parental genotype		Progeny genotype[a]			TE[b]	χ^2
Female	**Male**	***AtRH36-1/AtRH36-1***	***atrh36-1/AtRH36-1***	***arh36-1/atrh36-1***		
atrh36-1/AtRH36-1	*atrh36-1/AtRH36-1*	54.6% ($n = 53$)	45.4% ($n = 44$)	0% ($n = 0$)	83%	$P = 0.37$
atrh36-1/AtRH36-1	*AtRH36-1/AtRH36-1*	100% ($n = 296$)	0% ($n = 0$)	0% ($n = 0$)	0%	$P = 0.00$
AtRH36-1/AtRH36-1	*arh36-1/AtRH36-1*	55.8% ($n = 181$)	44.1% ($n = 143$)	0% ($n = 0$)	79%	$P = 0.03$

[a] Plants were crossed manually, and seeds of the crossed plants were collected and grown on Murashige and Skoog (MS) plates.
[b] Transmission efficiency (TE) = heterozygote/wild type × 100%.

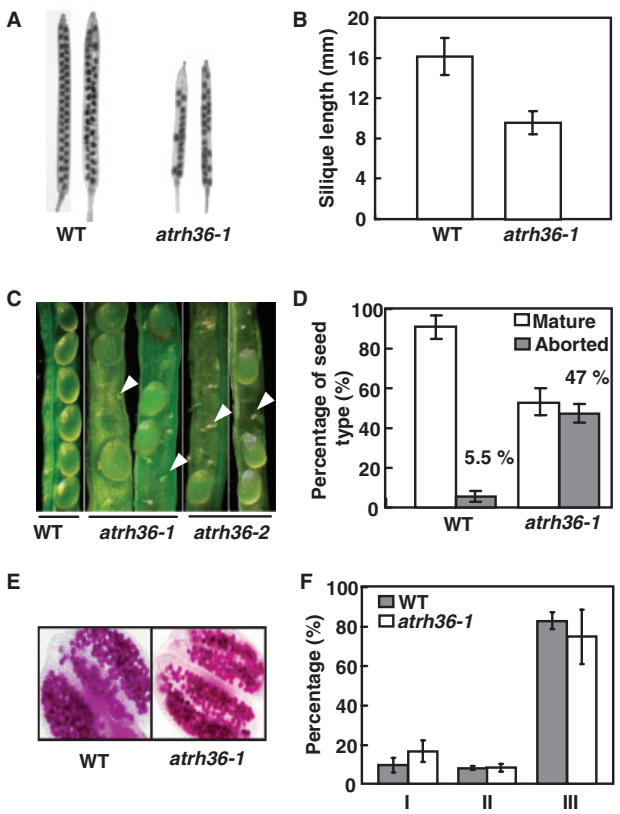

Fig. 3 Morphology of the *atrh36* heterozygous plants. (A and B) Silique morphology of self-pollinated wild-type and heterozygous mutant plants. Siliques from *atrh36-1* heterozygous plants were shorter than those of the wild type, and contained a reduced number of seeds. Error bars indicate the standard deviation. A total of 20 siliques were measured for wild-type and mutant plants. (C) Developing siliques produced from selfed heterozygotes contained more aborted seeds than those of the wild type. The aborted seeds are indicated by arrows. (D) The percentage of mature or aborted seeds in developing siliques. The percentage of mature seeds is represented by the white columns and aborted seeds by the gray columns. A total of 628 seeds were produced by wild-type plants and 1,178 by *atrh36-1* heterozygous plants. Error bars represent the standard deviation. (E) No obvious difference was found in pollen viability of wild-type and the *atrh36-1* heterozygous plants. Alexander staining was performed to indicate the viable pollen (red/purple) and dead pollen (green). (F) The pollen germination rate of the *atrh36-1* heterozygote was similar to that of the wild type. I, length of pollen tube >2-fold the length of pollen grain; II, length of pollen tube <2-fold the length of pollen grain; III, without germination.

To address further whether AtRH36 functions in male gametophyte development, the pollen viability of *atrh36-1* heterozygote plants was determined by Alexander staining. In **Fig. 3E**, no obvious difference was found in pollen morphology and pollen viability between the *atrh36-1* mutant and the wild type. Moreover, the pollen germination rates in *atrh36-1* heterozygote plants were similar to those of wild-type plants (**Fig. 3F**). Together, these results clearly indicated that mutation of *atrh36-1* affected female gametophyte development and slightly impaired male gametophyte development.

Ovules of the atrh36 mutant show a delayed progression in the female gametophytic cell cycle

The female gametophyte is generated from the functional megaspore via a process called megagametogenesis. Megagametogenesis begins with mitosis, cellularization and degeneration to develop a functional embryo sac that contains an egg cell, two synergid cells and a central cell. Christensen et al. (1998) have used confocal laser scanning microscopy (CLSM) to observe the process of megagametogenesis in Arabidopsis and have divided this process into eight stages: female gametophyte (FG) 1–FG8. To study how the *atrh36-1* mutation affects megagametogenesis, we performed CLSM to compare the progress of female gametophyte development in wild-type and *atrh36-1* heterozygous plants.

Eight stages of megagametogenesis were observed in wild-type plants by CLSM and are shown in **Fig. 4**. Often two or three sequential developmental stages predominate among ovules within the same pistil in Arabidopsis (**Table 3**). These results are consistent with the previous finding that the development of ovules within a pistil is synchronous in Arabidopsis (Christensen et al. 1997).

For the *atrh36-1* mutant, pistils were isolated from flower buds and analyzed by CLSM. The results showed that the development of most mutant embryo sacs was asynchronous (**Table 4**). Some female gametophytes within a single pistil spanned five or more developmental stages, such as Ps3–Ps6 shown in **Table 4**. For example, among 30 analyzed ovules from pistil 5 (PS5), four were at stage FG3 (**Fig. 5A**), eight were at stage FG4 (**Fig. 5B**), three were at stage FG5 (**Fig. 5C**), 11 were at stage FG6 (**Fig. 5D**) and four were at stage FG7 (**Fig. 5E**).

After manual pollination, embryogenesis was analyzed in wild-type and *atrh36-1* mutant plants. In selected wild-type pistils, all the developing seeds were at the zygote stage with

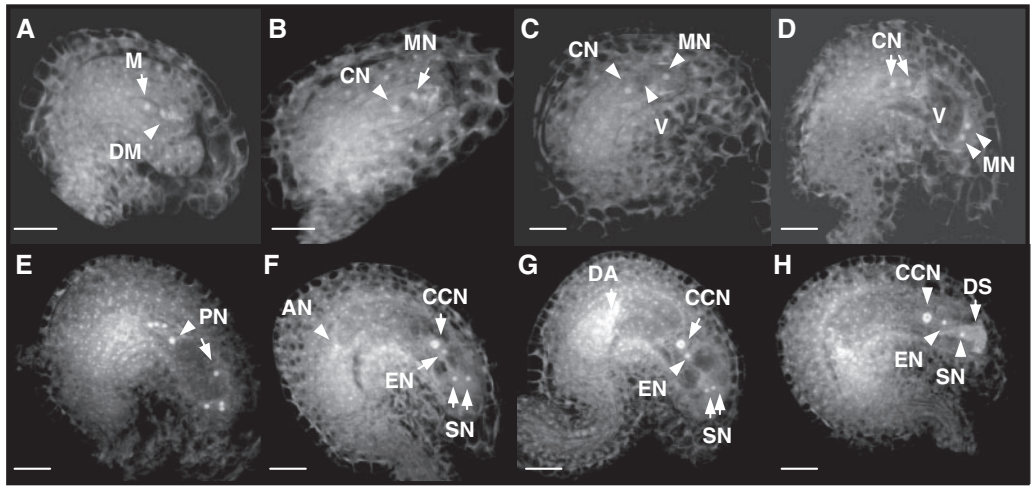

Fig. 4 CLSM observation of female gametophyte development in wild-type Arabidopsis. (A) An embryo sac at stage FG1. (B) An embryo sac at stage FG2. (C) An embryo sac at stage FG3. (D) An embryo sac at stage FG4. (E) An embryo sac at stage FG5. (F) An embryo sac at stage FG6. (G) An embryo sac at stage FG7. (H) An embryo sac at stage FG8 contained a three-celled female gametophyte. The degenerated synergid nuclei (DS) are indicated. All images were observed from multiple 1 µm optical sections under CLSM. M, teardrop-shaped megaspore; DM, degenerating megaspore; MN, micropylar nucleus; CN, chalazal nucleus; V, vacuole; PN, polar nucleus; CCN, central cell nucleus; SN, synergid nucleus; EN, egg nucleus; AN, antipodal nucleus; DA, degenerated antipodal nucleus; DS, degenerated synergid nucleus. Bars = 20 µm.

Table 3 Synchrony of female gametophyte development in wild-type Arabidopsis

Pistil number	No. of female gametophytes at developmental stages[a]								Total FGs
	FG1	FG2	FG3	FG4	FG5	FG6	FG7	Ed[b]	
Ps1	28	8							36
Ps2	2	6	24						32
Ps3		1	6	20					27
Ps4			7	17	4				28
Ps5					20	8			28
Ps6						5	22		27
Ps7						5	19		24
Ps8[c]								21	21
Ps9[c]								24	24

[a] Female gametophyte stages were according to Christensen et al. (1998).
[b] Embryo sacs containing 4- or 8-nucleate endosperm were grouped in Ed.
[c] The pistil was collected after 24 h of pollination.

Table 4 Synchrony of female gametophyte development in *atrh36-1* heterozygote Arabidopsis

Pistil number	No. of female gametophytes at developmental stages[a]								Total FGs
	FG1	FG2	FG3	FG4	FG5	FG6	FG7	Ed[b]	
Ps1	13	14							27
Ps2	5	11	11						27
Ps3	2	7	10	8	2				29
Ps4	2	4	4	11	11	1			33
Ps5			4	8	3	11	4		30
Ps6			1	4	12	5	9		31
Ps7[c]				3	9	6		16	34
Ps8[c]				9	3	1		6	19

[a] Female gametophyte stages were according to Christensen et al. (1998).
[b] Embryo sacs containing 4- or 8-nucleate endosperm were grouped in Ed.
[c] The pistil was collected after 24 h of pollination.

4- or 8-nucleate endosperm in the embryo sac (Ps8 and Ps9 in **Table 3**). However, in the pollinated *atrh36-1* pistils (Ps7 and Ps8 in **Table 4**), less than half the ovules developed into seeds that had 4-nucleate (**Fig. 5I**) or 8-nucleate (**Fig. 5J**) endosperm in the embryo sac; the rest of the ovules were still at stages FG4 (**Fig. 5F**), FG5 (**Fig. 5G**) and FG6 (**Fig. 5H**). Together, these results indicated that the *atrh36-1* mutant ovules showed a delayed progression in the female gametophytic cell cycle.

β-Estradiol-induced gene silencing of AtRH36 produces a pleiotropic phenotype in plant growth and results in the accumulation of rRNA precursors

To investigate the role of the *AtRH36* gene in whole plants, an inducible RNA interference (RNAi) approach was applied. A 500 bp fragment that corresponded to the 3′ end of the *AtRH36* cDNA was cloned in an inverted-repeat orientation that flanked a *GFP* DNA fragment (as a spacer), under the

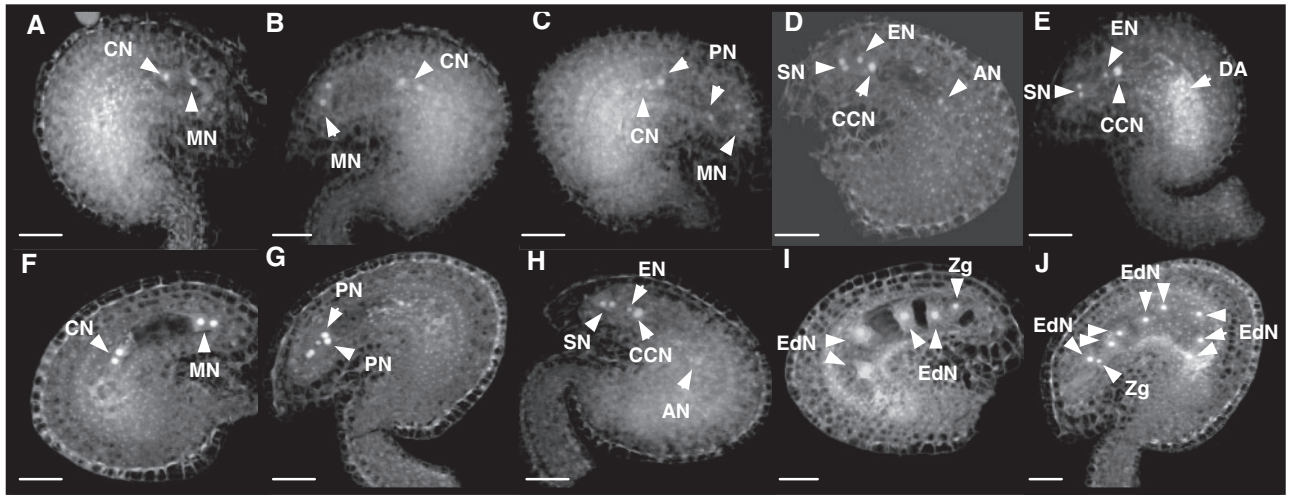

Fig. 5 Delayed cell cycle progression during female gametogenesis in pistils from *atrh36* heterozygous mutant plants. (A–E) Ovules were isolated from pistil 5 (Ps5) of an *atrh36-1* heterozygous mutant. (F–J) Approximately 24 h after pollination, ovules were isolated from pistil 7 (Ps7) of an *atrh36-1* heterozygous mutant. (A) Ovule with a 2-nucleate embryo sac at stage FG3. (B) Ovule with a 4-nucleate embryo sac at stage FG4. (C) Ovule with an 8-nucleate embryo sac at stage FG5. (D) Ovule with a 7-celled embryo sac at stage FG6. (E) Ovule with a 3-celled embryo sac at stage FG7. The degenerated antipodal nuclei (DA) exhibited strong autofluorescence. (F) Ovule with a 4-nucleate embryo sac at stage FG4. (G) Ovule with an 8-nucleate embryo sac at stage FG5. The two polar nuclei (PNs) migrated to form the central cell nucleus. (H) Ovule with a 7-celled embryo sac at stage FG6. (I) Fertilized ovule showing the second division of the endosperm nucleus (EdN). The zygote is shown (Zg). (J) Fertilized ovule showing the third division of the EdN. The Zg is indicated. All images were compiled from multiple 1 μm optical sections. AN, antipodal nucleus; CN, chahazal nucleus; CCN, central cell nucleus; DA, degenerated antipodal nucleus; EN, egg cell nucleus; EdN endosperm nucleus; MN, micropylar nucleus; PN, polar nucleus; SN, synergid nucleus; Zg, zygote nucleus. Bars = 20 μm.

control of a chimeric promoter that contained the *LexA* operator fused upstream to a minimal *35S* promoter (**Fig. 6A**). The RNAi construct and an effector plasmid, *35S::XVE*, were co-transformed into Arabidopsis. Under selection for kanamycin and hygromycin resistance, six independent transgenic plants (36Ri-1–36Ri-6) that contained both RNAi and effector T-DNA insertions were obtained and verified by genomic DNA PCR analysis. Ten-day-old transgenic seedlings were used to study the expression pattern of *AtRH36* and its downstream response. The accumulation of *AtRH36* mRNA was reduced dramatically in all the RNAi lines after treatment with β-estradiol, as compared with dimethylsulfoxide (DMSO; **Fig. 6B**). The root length of the seedlings was reduced significantly in all of the selected *AtRH36* knock-down lines, as compared with the wild-type and *35S::XVE* transgenic plants (**Fig. 6C**). To determine whether the short root phenotype observed in the *AtRH36* knockdown lines was caused by loss of cell viability, the 2,3,5-triphenyltetrazolium chloride (TTC) cell viability assay was performed. Cell viability in the root tip was reduced in the *AtRH36* knock-down lines, as compared with *35S::XVE* transgenic plants (**Supplementary Fig. S2**). To determine whether AtRH36 affects plant growth and development, seeds from the wild type and from the *AtRH36* knockdown lines 36Ri-2 and 36Ri-5 were germinated in 1/2 Murashige and Skoog (MS) medium with either β-estradiol or DMSO, and their phenotypes were compared. Seed germination and seedling growth were retarded only in β-estradiol-treated transgenic lines (36Ri-2 and 36Ri-5), but not in wild-type and *35S::XVE* transgenic plants (**Fig. 6D**). In addition, when the 2-week-old 36Ri-5 plants were shifted to medium that contained β-estradiol, short roots, abnormal leaves, accumulation of anthocyanin, delayed reproductive transition and early senescence were observed, as compared with treatment with DMSO (**Fig. 6E**). Overall, these results indicate that AtRH36 is required for plant growth and development.

In eukaryotic cells, transcription of rDNA generates a 45S rRNA precursor, which comprises 5′ ETS–18S rRNA–ITS1–5.8S rRNA–ITS2–25S rRNA–3′ ETS (ETS, external transcribed sequence; ITS, internal transcribed sequence). 18S, 5.8S and 25S rRNA are formed by cleavage of the 45S rRNA precursor (**Fig. 7A**). To determine whether AtRH36 plays a role in Arabidopsis rRNA maturation, the rRNA precursor was analyzed in *AtRH36* knock-down lines. Ten-day-old wild-type, 36Ri-2, 36Ri-3 and 36Ri-5 plants were transferred for 5 d to medium that contained either β-estradiol or DMSO. Total RNA was isolated from the roots of each individual line and RT–PCR was performed to evaluate the abundance of the rRNA precursor. Under β-estradiol treatment, the expression of *AtRH36* was knocked down significantly, and the level of the rRNA precursor (amplified using two specific primer sets, U2 with U3 and IS1 with IS2) was increased in all three β-estradiol-inducible RNAi plants, as compared with the wild type (**Fig. 7B**). The specific primers 18SF and 18SR were used to show that an equal amount of total 18S rRNA, which included the mature and immature forms of 18S, was included

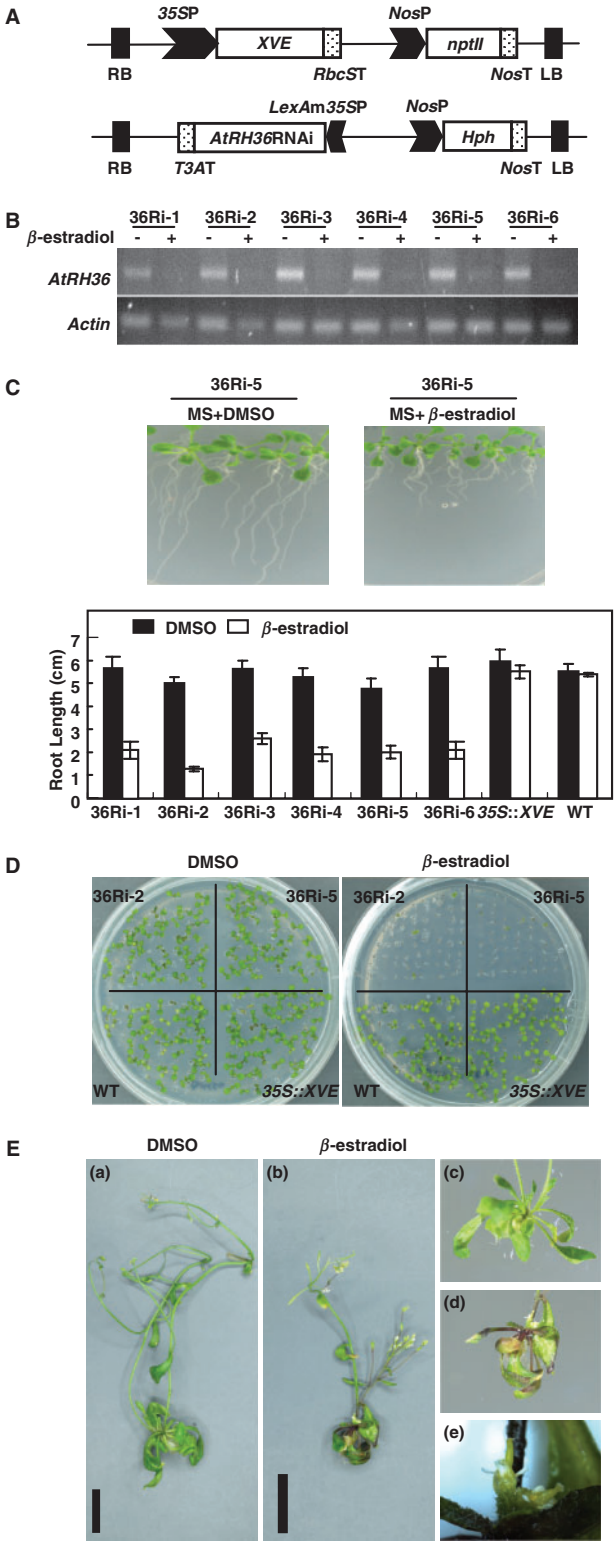

Fig. 6 Inducible knockdown of *AtRH36* expression resulted in pleiotropic phenotypes during plant growth. (A) Schematic representations of an effector vector that contained the *35S::XVE* gene and an inducible RNAi expression vector that contained *AtRH36RNAi*. A chimeric transcription factor *XVE* gene was under the control of the *CaMV35S* promoter (*35SP*) and the ribulose-1,5-bisphosphate carboxylase/oxygenase small subunit terminator (*Rbc*ST). The DNA fragment of *AtRH36* RNAi was under the control of the chimeric *LexA*m*35S* promoter and the *T3A* terminator (*T3AT*). The kanamycin resistance gene (*nptII*) and hygromycin resistance gene (*Hph*) were driven by the nopaline synthase promoter (*Nos*P) and terminated by the nopaline synthase terminator (*Nos*T). Constructs contained the left and right borders (LB and RB). (B) RT–PCR analysis of *AtRH36* expression in six independent inducible RNAi lines. Ten-day-old plants were incubated with 10 μM β-estradiol (+) or DMSO (–) for 7 d. Total RNA was purified and subjected to RT–PCR using primers specific for *AtRH36* and *Actin* (internal control). (C) Root phenotype of inducible RNAi plants. Ten-day-old plants were incubated with either 10 μM DMSO or β-estradiol (inducer for RNAi lines) in MS medium for 7 d. Root morphorgy of an RNAi line, 36Ri5, is shown in the upper panel. Statistical comparison of root length is shown in the lower panel. Error bars represent the standard deviation ($n > 10$). (D) Comparison of seed germination among WT, *35S::XVE*, 36Ri-2 and 36Ri-5 treated with β-estradiol or DMSO. (E) Comparison of a 30-day-old RNAi line, 36Ri-5, treated with DMSO (a) or β-estradiol (b). Leaf morphology, DMSO (c) or β-estradiol (d) treated. Flower morphology of the β-estradiol-treated 36Ri-5 line (e).

in all the PCRs. The *Actin* gene was used as a loading control for the PCR analysis (**Figure 7B**). Knock-down of *AtRH36* expression resulted in accumulation of immature rRNA precursor, which suggested that AtRH36 participates in the processing of 18S rRNA in Arabidopsis.

Discussion

In this study, we identified the *AtRH36* gene from Arabidopsis, and characterized the phenotypes of *atrh36* mutants. We showed that AtRH36 was homologous to the yeast DEAD-box protein Dbp8p, which is required for ribosome biogenesis. DEAD-box proteins are thought to function in ribosome biogenesis, and have been proposed to share a highly conserved mechanism of action among eukaryotes (Mingam et al. 2004, Linder 2006). In yeast, Dbp8p is localized to the nucleolus and is essential for viability. Depletion of Dbp8p leads to decreased levels of the small ribosomal subunit as a result of the absence of cleavage at sites A_0, A_1 and A_2 during rRNA processing (Daugeron and Linder 2001). In this study, we showed that homozygosity for *atrh36-1* and *atrh36-2* could not be obtained, which suggests that *AtRH36* is important in plants. Detailed analysis of *AtRH36* knock-down plants showed that AtRH36 is involved at an early stage of rRNA processing. The results of our studies also indicated that AtRH36 was localized predominantly to the nucleus and accumulated in the nucleolus. Consistent with the function of Dbp8p in yeast, our findings provide further biological evidence that DEAD-box proteins are also involved in ribosome biogenesis in plants.

The present study showed that female mitotic progression was retarded significantly in the *atrh36-1* heterozygous mutant, and demonstrated the important physiological role of AtRH36 in Arabidopsis. A similar study investigated the *swa1* (*slow walker 1*) and *swa2* mutants in Arabidopsis (Shi et al. 2005,

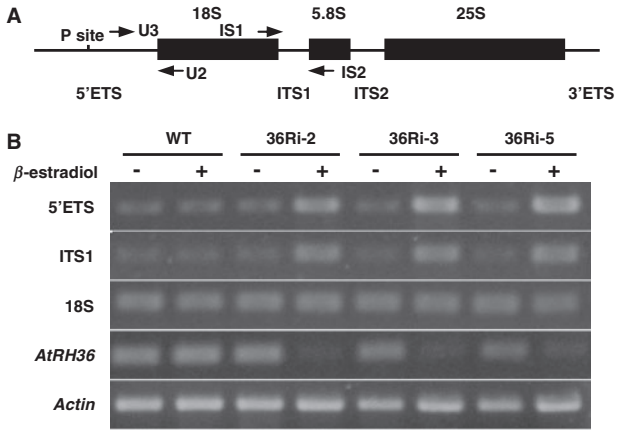

Fig. 7 *AtRH36* participates in the processing of 45S pre-rRNA in Arabidopsis. (A) Structure of Arabidopsis pre-rRNA transcript, which contained the 5′ ETS, 18S rRNA (18S), ITS1, 5.8S rRNA (5.8S), ITS2, 25S rRNA (25S) and 3′ ETS. The P site, which is located at position +1,275 in 45S rRNA, is known as the primary cleavage site for rRNA maturation in Arabidopsis (Saez-Vasquez et al. 2004). The primers U2 and U3 are designed to detect the 5′ ETS, and primers IS1 and IS2 to detect ITS1. (B) Ten-day-old wild-type (WT) and three RNAi lines, 36Ri-2, 36Ri-3 and 36Ri-5, were incubated with 10 μM β-estradiol (+) or DMSO (−). Total RNA was purified and subjected to RT–PCR using primers specific for 5′ ETS, ITS1, 18S, *AtRH36* and *Actin* (internal control).

Li et al. 2009). *SWA1* encodes a nucleolar protein with six WD40-repeat motifs and is homologous to yeast Utp15, which is a component of a nucleolar U3 complex that is required for rRNA biogenesis. Knock-down of *SWA1* expression leads to the accumulation of a significant amount of unprocessed pre-18S rRNA. SWA2 contains a DEXDc domain and is homologous to yeast NOC1/MAK21, which is involved in ribosome biogenesis and the export of pre-ribosomes from the nucleus to the cytoplasm. The embryo sacs from both *swa1* and *swa2* mutants have aberrant mitotic division cycles and show asynchronous female gametogenesis. In addition, mutations in a number of genes that are possibly related to rRNA biogenesis, which include *UTP11* (At3g60630), *NOP11p* (At2g20490), *AtSYN3* (At3g59550), *DOMINO1* (At5g62440), *TORMOZ* (At5g16750) and a *Sen1* homolog (*MAA3*, At4g15570), also impair female gametogenesis (Lahmy et al. 2004, Pagnussat et al. 2005, Griffith et al. 2007, Jiang et al. 2007, Shimizu et al. 2008). For example, fusion of polar nuclei in the embryo sacs of the *maa3* mutant is aberrant, which results in arrest or delay in the progression of female mitotic division. The mutant phenotype of *maa3* is very similar to that of our *atrh36-1* mutant, which also shows defects in rRNA biogenesis, and abnormal mitotic cycles during female gametogenesis. Therefore, it seems that the abnormal biogenesis of rRNA affects mitotic cycles by interfering directly with cell cycle-related proteins. Another finding that supports the idea is the mutation of *NOMEGA*, which encodes the APC6/cell division cycle (CDC) 16 subunit of the anaphase-promoting complex (APC). In the presence of this mutation, cyclin B cannot be degraded, hence 30% of embryo sacs are arrested at the 2-nucleate stage (Kwee and Sundaresan 2003). However, the results of the current study do not rule out the possibility that AtRH36 has a special role in female gametogenesis, which might not be related to its function in rRNA biogenesis.

In Arabidopsis, pollen is produced through diploid pollen mother cells undergoing meiosis and two mitotic divisions in the anther. Although the transmission rate of the *atrh36-1* mutant allele was slightly affected, there was no obvious difference in the morphology, viability and germination rate of pollen grains between *atrh36-1* heterozygous and wild-type plants. Our findings are consistent with a previous study showing that a defect in rRNA biogenesis requiring the *swa1* gene only affects female gametophyte development (Shi et al. 2005). It suggests that although rRNA biogenesis is a general process for mitotic division in male and female gametophyte development, defects in rRNA biogenesis might not affect the post-meiosis stage of male gametogenesis. Maternal rRNA has been detected in the microspores of tobacco (Saito et al. 1998); therefore, two mitotic divisions could be supported sufficiently by residual rRNA after meiosis in microgametogenesis. Another possibility is that a microspore could contain enough maternal AtRH36 activity to support de novo rRNA synthesis for pollen grains to mature. Thirdly, although we have shown that the *AtRH36* promoter has slight activity in the pollen tube, the expression of *AtRH36* is very low in the pollen grains from microarray data available at GENEVESTIGATOR (https://www.genevestigator.ethz.ch) (data not shown). Therefore, AtRH36 may not play a role in pollen development and could be be replaced by genetic redundancy.

Severe effects on root growth, transition to reproductive growth and mature leaf chlorosis were found in transgenic Arabidopsis plants in which *AtRH36* had been knocked down. In addition, RT–PCR and the promoter::*GUS* reporter system revealed that *AtRH36* was expressed ubiquitously in all tissues throughout plant development. Taken together, these results suggest that AtRH36 has a global effect on plant development through its involvement in rRNA biogenesis, and elimination of AtRH36 results in morphological changes in different organs. It can be argued that ribosome biogenesis is the most important cellular process, because ribosomes are responsible for the translation of mRNA into protein (Tushinski and Warner 1982, Mager 1988). Several genetic studies have shown that mutations in genes for ribosomal proteins and proteins involved in ribosome biogenesis reduce cell division, retard growth, cause morphological abnormalities and result in a late-flowering phenotype (Van Lijsebettens et al. 1994, Ito et al. 2000, Popescu and Tumer 2004, Kojima et al. 2007, Petricka and Nelson 2007, Pinon et al. 2008, Yao et al. 2008, Fujikura et al. 2009). Perturbations in ribosomal processing usually lead to alterations in plant morphology, and this phenomenon is usually related to sugars (Kojima et al. 2007). It is known that sugar can enhance expression of a large number of genes for ribosomal proteins and proteins which function in ribosome synthesis. For example, nucleolin is a global regulator of ribosome synthesis

(Tuteja and Tuteja 1998, Srivastava and Pollard 1999). One of the nuceolins in Arabidopsis is encoded by *AtNuc-L1*, and expression of this gene is strongly induced by sucrose and glucose. Mutation of *AtNuc-L1* caused an increased level of pre-rRNA and aberrations in plant morphology (Kojima et al. 2007). These findings suggest that sugar regulates the expression level of *AtRH36* to adjust the maturation of rRNA, and therefore expression of *AtRH36* plays a critical role through the influence of rRNA on multiple developmental pathways. Further research might explore how AtRH36 functions during plant growth and development.

In summary, our data demonstrated the function of AtRH36 in rRNA biogenesis in plants. Moreover, AtRH36 is essential for the mitotic division cycles that occur during female gametogenesis and is important for growth and development in Arabidopsis.

Materials and Methods

Plant materials

We obtained the T-DNA insertion mutants *atrh36-1* (SALK_102486), *atrh36-2* (SALK_079348) and *atrh36-3* (SALK_045190) in the Arabidopsis ecotype Col-0 from the Salk Institute Genomic Analysis Laboratory (SIGnAL) through the Arabidopsis Biological Resource Center (ABRC). Arabidopsis seeds were surface sterilized, incubated at 4°C for 4 d, plated on 1/2 MS medium that contained 0.8% agar supplemented with 1% sucrose, and grown at 22°C under a 16 h light/8 h dark photoperiod.

Primers

All primers used in this study are listed in **Supplementary Table S1**.

Isolation of AtRH36 cDNA

Total RNA was prepared from 2-week-old Arabidopsis seedlings. First-strand cDNA was synthesized from total RNA using SuperScript III Reverse Transcriptase (Invitrogen, Carlsbad, CA, USA). The full-length *AtRH36* cDNA (1,476 bp) was generated by RT–PCR and inserted into the *Bam*HI and *Sac*I sites in pBluescript KS+ to give pBSAtRH36.

Plasmids

The pMDC vector series was a gift from Mark Curtis (Brand et al. 2006, Jia et al. 2007). The pCAMBIA vector series was obtained from Cambia (www.cambia.org).

To make the construct for complementation of the *atrh36-1* phenotype, the genomic DNA region of *AtRH36* from 469 bp upstream of the start codon to 280 bp downstream of the stop codon was isolated by PCR using Arabidopsis genomic DNA as the template. The resulting PCR product was cloned into a pyT&A cloning vector (Yeastern Biotech, Taipei, Taiwan) to generate pAtRH36g. pAtRH36g was digested with *Bam*HI and *Sac*I, and ligated into the binary vector pCAMBIA-1301 to generate p1301AtRH36g.

For the AtRH36–GFP fusion construct, the primers AtRH36GF and AtRH36GR were used to amplify *AtRH36* cDNA. The resulting PCR product was inserted into the vector pENTR/SD/D-TOPO (Invitrogen, Carlsbad, CA, USA) to generate the construct pENTR-AtRH36. pENTR-AtRH36 was used to subclone the AtRH36 cDNA into the destination vector pMDC83 (Curtis and Grossniklaus 2003) by LR recombination (Invitrogen, Carlsbad, CA, USA), which generated p35SAtRH36-GFP.

To synthesize the *AtRH36::GUS* reporter construct, the 469 bp promoter region of *AtRH36* was amplified by PCR using the primers AtRH36p-F and AtRH36p-R. The resulting PCR product was digested with *Bam*HI and *Nco*I, and ligated into pCAMBIA-1305 to generate p1305AtRH36GUS.

To make the AtRH36 RNAi construct, pBSAtRH36 was digested with *Sac*I and *Eco*RI to isolate the 500 bp 3′ end of the *AtRH36* cDNA, ligated as inverted repeats either side of the coding sequence for GFP (as a spacer) and then ligated into pBluescript KS+, to generate pAtRH36RNAi. The 1.7 kb AtRH36RNAi DNA fragment was amplified by PCR with the primer AtRH36RNAi-Topo, and inserted into the pENTR/SD/D-TOPO vector, to generate the construct pENTR-AtRH36RNAi. pENTR-AtRH36RNAi was used to subclone the AtRH36RNAi DNA fragment into the destination vector pMDC221(Brand et al. 2006) by LR recombination, which generated pLexAAtRH36Ri. For the *35SE::XVE* effector construct, the *35S* enhancer DNA fragment was amplified using primers 35Se F and 35Se R, and inserted into the pENTR/SD/D-TOPO vector to generate pENTR35SEN. pENTR35SEN was used to subclone the *35S* enhancer DNA fragment into the destination vector pMDC150 (Brand et al. 2006) by LR recombination, which generated p35SXVE.

Transformation of plants

Plasmids were introduced into *Agrobacterium tumefaciens* strain GV3101 by electroporation. *Arabidopsis thaliana* plants (Col-0 or *atrh36-1* heterozygous mutant) were transformed using a floral dip method (Clough and Bent 1998). Progeny seedlings were selected on MS medium that contained 30 mg l^{-1} hygromycin for plants transformed with p1301AtRH36g and with p1305AtRH36GUS, and 25 mg l^{-1} hygromycin plus 70 mg l^{-1} kanamycin for plants co-transformed with pLexAAtRH36Ri and p35SXVE.

Analysis of promoter activity and nuclear localization

Organs at different developmental stages were harvested from transgenic plants that contained the *AtRH36* promoter-driven *GUS* expression cassette, for analysis of GUS activity. The various organs were incubated in GUS staining solution at 37°C overnight, as described by Jefferson et al. (1987). Chlorophyll was then removed with 95% ethanol. The organs were observed and photographed using an Olympus IX71 inverted microscope with a digital camera.

The onion bulb epidermis was prepared and particle bombardment was carried out as described by Scott et al. (1999) to introduce p35SGFP (a plasmid containing *35S* promoter::*GFP*; a gift from S.-M. Yu) or p35SAtRH36-GFP using a PDS-1000 biolistic device (Bio-Rad, Hercules, CA, USA) at 1,100 p.s.i. Bombarded specimens were incubated in MS medium for 2 d, and were then observed with an Olympus IX71 inverted fluorescence microscope.

Characterization of the atrh36-1, atrh36-2 and atrh36-3 alleles and segregation analysis

The presence of the T-DNA insertion in the *atrh36-1*, *atrh36-2* and *atrh36-3* mutants was verified by PCR using the T-DNA left border primer LBa1 and the *AtRH36* gene-specific primers 36-1R and 36-1L for *atrh36-1* and *atrh36-2*, and 36-3R and 36-3L for *atrh36-3*. To analyze progeny from self-crossing, heterozygous plants were allowed to self-pollinate, and the genotypes of the progeny plants were analyzed. To analyze reciprocal crosses, the wild type (Ler ecotype) or *atrh36-1* heterozygotes (Col-0 ecotype) as the female parent were crossed with *atrh36-1* or the wild type, respectively, as the male parent. Seeds from different siliques were collected and plated on MS medium. The genotypes of the seedlings were analyzed by PCR.

RT–PCR

Total RNA was extracted from wild-type and transgenic plants using TRIzol reagent (Invitrogen, Carlsbad, CA, USA). Possible DNA contamination was removed using RNase-free DNase (Ambion, Austin, TX, USA). First-strand cDNA synthesis was primed with an oligo(dT) primer and catalyzed by SuperScript III Reverse Transcriptase (Invitrogen, Carlsbad, CA, USA). A 50-fold dilution of the first-strand cDNA was then subjected to PCR with gene-specific primers. A total of 22–28 reaction cycles of PCR amplification were performed. For the detection of pre-rRNA, first-strand cDNA synthesis was primed with random primers (Invitrogen, Carlsbad, CA, USA) and catalyzed by SuperScript III Reverse Transcriptase (Invitrogen, Carlsbad, CA, USA). The first-strand cDNA was diluted 500-fold and then subjected to PCR with primers designed to detect specific processing of rRNA. The primers 18SF and 18SR were designed to detect total 18S rRNA, including mature 18S rRNA and 18S pre-rRNA. The primers U2 and U3 were designed to bind downstream of the P site to analyze the removal of the 5′ ETS from the pre-rRNA. The primers IS1 and IS2 were designed to analyze the removal of the ITS from the pre-rRNA.

CLSM

Confocal observation of the stages of female gametophyte development was performed as described by Christensen et al. (1998), with the modification that we used a Zeiss LSM510 microscope. Primary inflorescences were isolated from Col-0 and *atrh36-1* heterozygous plants to identify the female gametophyte phenotype. Pistils from the same inflorescence were collected, fixed, and opened to dissect out ovules. Ovules were cleared in 2 : 1 (v/v) benzyl benzoate : benzyl alcohol and sealed under coverslips. The number of nuclei in the ovules of Col-0 and *atrh36-1* plants was determined by analyzing serial optical sections of images captured on a Zeiss LSM510 microscope with Zeiss LSM Image Browser software.

Supplementary data

Supplementary data are available at PCP online.

Funding

This work was supported by the National Science Council of the Republic of China [grant 98-2311-B-008-002-MY3].

Acknowledgments

We thank Dr. Su-May Yu and Ms. Sue-Ping Lee at Institute of Molecular Biology, Academia Sinica, Taipei, for technical assistance with confocal microscopy.

References

Aubourg, S., Kreis, M. and Lecharny, A. (1999) The DEAD box RNA helicase family in Arabidopsis thaliana. *Nucleic Acids Res.* 27: 628–636.

Boudet, N., Aubourg, S., Toffano-Nioche, C., Kreis, M. and Lecharny, A. (2001) Evolution of intron/exon structure of DEAD helicase family genes in Arabidopsis, Caenorhabditis, and *Drosophila*. *Genome Res.* 11: 2101–2114.

Brand, L., Horler, M., Nuesch, E., Vassalli, S., Barrell, P., Yang, W., et al. (2006) A versatile and reliable two-component system for tissue-specific gene induction in Arabidopsis. *Plant Physiol.* 141: 1194–1204.

Chen, J.Y., Stands, L., Staley, J.P., Jackups, R.R., Jr., Latus, L.J. and Chang, T.H. (2001) Specific alterations of U1-C protein or U1 small nuclear RNA can eliminate the requirement of Prp28p, an essential DEAD box splicing factor. *Mol Cell* 7: 227–232.

Christensen, C.A., King, E.J., Jordan, J.R. and Drews, G.N. (1997) Megagametogenesis in Arabidopsis wild type and the Gf mutant. *Sex. Plant Reprod.* 10: 49–64.

Christensen, C.A., Subramanian, S. and Drews, G.N. (1998) Identification of gametophytic mutations affecting female gametophyte development in Arabidopsis. *Dev. Biol.* 202: 136–151.

Clough, S.J. and Bent, A.F. (1998) Floral dip: a simplified method for Agrobacterium-mediated transformation of Arabidopsis thaliana. *Plant J.* 16: 735–743.

Cordin, O., Banroques, J., Tanner, N.K. and Linder, P. (2006) The DEAD-box protein family of RNA helicases. *Gene* 367: 17–37.

Curtis, M.D. and Grossniklaus, U. (2003) A gateway cloning vector set for high-throughput functional analysis of genes in planta. *Plant Physiol.* 133: 462–469.

Daugeron, M.C. and Linder, P. (2001) Characterization and mutational analysis of yeast Dbp8p, a putative RNA helicase involved in ribosome biogenesis. *Nucleic Acids Res.* 29: 1144–1155.

de la Cruz, J., Kressler, D. and Linder, P. (1999) Unwinding RNA in *Saccharomyces cerevisiae*: DEAD-box proteins and related families. *Trends Biochem. Sci.* 24: 192–198.

Fujikura, U., Horiguchi, G., Ponce, M.R., Micol, J.L. and Tsukaya, H. (2009) Coordination of cell proliferation and cell expansion mediated by ribosome-related processes in the leaves of Arabidopsis thaliana. *Plant J.* 59: 499–508.

Gendra, E., Moreno, A., Alba, M.M. and Pages, M. (2004) Interaction of the plant glycine-rich RNA-binding protein MA16 with a novel nucleolar DEAD box RNA helicase protein from Zea mays. *Plant J.* 38: 875–886.

Gong, Z., Dong, C.H., Lee, H., Zhu, J., Xiong, L., Gong, D., et al. (2005) A DEAD box RNA helicase is essential for mRNA export and important for development and stress responses in Arabidopsis. *Plant Cell* 17: 256–267.

Griffith, M.E., Mayer, U., Capron, A., Ngo, Q.A., Surendrarao, A., McClinton, R., et al. (2007) The TORMOZ gene encodes a nucleolar protein required for regulated division planes and embryo development in Arabidopsis. *Plant Cell* 19: 2246–2263.

Ito, T., Kim, G.T. and Shinozaki, K. (2000) Disruption of an Arabidopsis cytoplasmic ribosomal protein S13-homologous gene by transposon-mediated mutagenesis causes aberrant growth and development. *Plant J.* 22: 257–264.

Jacobsen, S.E., Running, M.P. and Meyerowitz, E.M. (1999) Disruption of an RNA helicase/RNase III gene in Arabidopsis causes unregulated cell division in floral meristems. *Development* 126: 5231–5243.

Jefferson, R.A., Kavanagh, T.A. and Bevan, M.W. (1987) GUS fusions: beta-glucuronidase as a sensitive and versatile gene fusion marker in higher plants. *EMBO J.* 6: 3901–3907.

Jia, H., Van Loock, B., Liao, M., Verbelen, J.P. and Vissenberg, K. (2007) Combination of the ALCR/alcA ethanol switch and GAL4/VP16-UAS enhancer trap system enables spatial and temporal control of transgene expression in Arabidopsis. *Plant Biotechnol. J.* 5: 477–482.

Jiang, L., Xia, M., Strittmatter, L.I. and Makaroff, C.A. (2007) The Arabidopsis cohesin protein SYN3 localizes to the nucleolus and is essential for gametogenesis. *Plant J.* 50: 1020–1034.

Kant, P., Kant, S., Gordon, M., Shaked, R. and Barak, S. (2007) STRESS RESPONSE SUPPRESSOR1 and STRESS RESPONSE SUPPRESSOR2, two DEAD-box RNA helicases that attenuate Arabidopsis responses to multiple abiotic stresses. *Plant Physiol.* 145: 814–830.

Kim, J.S., Kim, K.A., Oh, T.R., Park, C.M. and Kang, H. (2008) Functional characterization of DEAD-box RNA helicases in Arabidopsis thaliana under abiotic stress conditions. *Plant Cell Physiol.* 49: 1563–1571.

Kistler, A.L. and Guthrie, C. (2001) Deletion of MUD2, the yeast homolog of U2AF65, can bypass the requirement for sub2, an essential spliceosomal ATPase. *Genes Dev.* 15: 42–49.

Kojima, H., Suzuki, T., Kato, T., Enomoto, K., Sato, S., Tabata, S., et al. (2007) Sugar-inducible expression of the nucleolin-1 gene of Arabidopsis thaliana and its role in ribosome synthesis, growth and development. *Plant J.* 49: 1053–1063.

Kwee, H.S. and Sundaresan, V. (2003) The NOMEGA gene required for female gametophyte development encodes the putative APC6/CDC16 component of the anaphase promoting complex in Arabidopsis. *Plant J.* 36: 853–866.

Lahmy, S., Guilleminot, J., Cheng, C.M., Bechtold, N., Albert, S., Pelletier, G., et al. (2004) DOMINO1, a member of a small plant-specific gene family, encodes a protein essential for nuclear and nucleolar functions. *Plant J.* 39: 809–820.

Li, D., Liu, H., Zhang, H., Wang, X. and Song, F. (2008) OsBIRH1, a DEAD-box RNA helicase with functions in modulating defence responses against pathogen infection and oxidative stress. *J. Exp. Bot.* 59: 2133–2146.

Li, N., Yuan, L., Liu, N., Shi, D., Li, X., Tang, Z., et al. (2009) SLOW WALKER2, a NOC1/Mak21 homologue, is essential for coordinated cell cycle progression during female gametophyte development in Arabidopsis. *Plant Physiol.* 151: 1486–1497.

Li, S.C., Chung, M.C. and Chen, C.S. (2001) Cloning and characterization of a DEAD box RNA helicase from the viable seedlings of aged mung bean. *Plant Mol. Biol.* 47: 761–770.

Linder, P. (2006) Dead-box proteins: a family affair—active and passive players in RNP-remodeling. *Nucleic Acids Res.* 34: 4168–4180.

Linder, P., Gasteiger, E. and Bairoch, A. (2000) A comprehensive web resource on RNA helicases from the baker's yeast *Saccharomyces cerevisiae*. *Yeast* 16: 507–509.

Linder, P. and Lasko, P. (2006) Bent out of shape: RNA unwinding by the DEAD-box helicase Vasa. *Cell* 125: 219–221.

Linder, P. and Owttrim, G.W. (2009) Plant RNA helicases: linking aberrant and silencing RNA. *Trends Plant Sci.* 14: 344–352.

Mager, W.H. (1988) Control of ribosomal protein gene expression. *Biochim. Biophys. Acta* 949: 1–15.

Matthes, A., Schmidt-Gattung, S., Kohler, D., Forner, J., Wildum, S., Raabe, M., et al. (2007) Two DEAD-box proteins may be part of RNA-dependent high-molecular-mass protein complexes in Arabidopsis mitochondria. *Plant Physiol.* 145: 1637–1646.

Mingam, A., Toffano-Nioche, C., Brunaud, V., Boudet, N., Kreis, M. and Lecharny, A. (2004) DEAD-box RNA helicases in Arabidopsis thaliana: establishing a link between quantitative expression, gene structure and evolution of a family of genes. *Plant Biotechnol. J.* 2: 401–415.

Okanami, M., Meshi, T. and Iwabuchi, M. (1998) Characterization of a DEAD box ATPase/RNA helicase protein of Arabidopsis thaliana. *Nucleic Acids Res.* 26: 2638–2643.

Pagnussat, G.C., Yu, H.J., Ngo, Q.A., Rajani, S., Mayalagu, S., Johnson, C.S., et al. (2005) Genetic and molecular identification of genes required for female gametophyte development and function in Arabidopsis. *Development* 132: 603–614.

Park, W., Li, J., Song, R., Messing, J. and Chen, X. (2002) CARPEL FACTORY, a Dicer homolog, and HEN1, a novel protein, act in microRNA metabolism in Arabidopsis thaliana. *Curr. Biol.* 12: 1484–1495.

Petricka, J.J. and Nelson, T.M. (2007) Arabidopsis nucleolin affects plant development and patterning. *Plant Physiol.* 144: 173–186.

Pinon, V., Etchells, J.P., Rossignol, P., Collier, S.A., Arroyo, J.M., Martienssen, R.A., et al. (2008) Three PIGGYBACK genes that specifically influence leaf patterning encode ribosomal proteins. *Development* 135: 1315–1324.

Popescu, S.C. and Tumer, N.E. (2004) Silencing of ribosomal protein L3 genes in N. tabacum reveals coordinate expression and significant alterations in plant growth, development and ribosome biogenesis. *Plant J.* 39: 29–44.

Pyle, A.M. (2008) Translocation and unwinding mechanisms of RNA and DNA helicases. *Annu. Rev. Biophys.* 37: 317–336.

Pyle, A.M., Fedorova, O. and Waldsich, C. (2007) Folding of group II introns: a model system for large, multidomain RNAs? *Trends Biochem. Sci.* 32: 138–145.

Rocak, S. and Linder, P. (2004) DEAD-box proteins: the driving forces behind RNA metabolism. *Nat. Rev. Mol. Cell Biol.* 5: 232–241.

Saez-Vasquez, J., Caparros-Ruiz, D., Barneche, F. and Echeverria, M. (2004) A plant snoRNP complex containing snoRNAs, fibrillarin, and nucleolin-like proteins is competent for both rRNA gene binding and pre-rRNA processing in vitro. *Mol. Cell. Biol.* 24: 7284–7297.

Saito, C., Fujie, M., Sakai, A., Kuroiwa, H, and Kuroiwa, T. (1998) Detection and quantification of rRNA by high-resolution in situ hybridization in pollen grains. *J. Plant Res.* 111: 45–52.

Scott, A., Wyatt, S., Tsou, P.L., Robertson, D. and Allen, N.S. (1999) Model system for plant cell biology: GFP imaging in living onion epidermal cells. *Biotechniques* 26: 1125, 1128–1132.

Sengoku, T., Nureki, O., Nakamura, A., Kobayashi, S. and Yokoyama, S. (2006) Structural basis for RNA unwinding by the DEAD-box protein *Drosophila* Vasa. *Cell* 125: 287–300.

Shi, D.Q., Liu, J., Xiang, Y.H., Ye, D., Sundaresan, V. and Yang, W.C. (2005) SLOW WALKER1, essential for gametogenesis in Arabidopsis, encodes a WD40 protein involved in 18S ribosomal RNA biogenesis. *Plant Cell* 17: 2340–2354.

Shimizu, K.K., Ito, T., Ishiguro, S. and Okada, K. (2008) MAA3 (MAGATAMA3) helicase gene is required for female gametophyte development and pollen tube guidance in Arabidopsis thaliana. *Plant Cell Physiol.* 49: 1478–1483.

Srivastava, M. and Pollard, H.B. (1999) Molecular dissection of nucleolin's role in growth and cell proliferation: new insights. *FASEB J.* 13: 1911–1922.

Stonebloom, S., Burch-Smith, T., Kim, I., Meinke, D., Mindrinos, M. and Zambryski, P. (2009) Loss of the plant DEAD-box protein ISE1 leads to defective mitochondria and increased cell-to-cell transport via plasmodesmata. *Proc. Natl Acad. Sci. USA* 106: 17229–17234.

Tanner, N.K. and Linder, P. (2001) DExD/H box RNA helicases: from generic motors to specific dissociation functions. *Mol. Cell* 8: 251–262.

Tushinski, R.J. and Warner, J.R. (1982) Ribosomal proteins are synthesized preferentially in cells commencing growth. *J. Cell Physiol.* 112: 128–135.

Tuteja, R. and Tuteja, N. (1998) Nucleolin: a multifunctional major nucleolar phosphoprotein. *Crit. Rev. Biochem. Mol. Biol.* 33: 407–436.

Van Lijsebettens, M., Vanderhaeghen, R., De Block, M., Bauw, G., Villarroel, R. and Van Montagu, M. (1994) An S18 ribosomal protein gene copy at the Arabidopsis PFL locus affects plant development by its specific expression in meristems. *EMBO J.* 13: 3378–3388.

Wang, Y., Duby, G., Purnelle, B. and Boutry, M. (2000) Tobacco VDL gene encodes a plastid DEAD box RNA helicase and is involved in chloroplast differentiation and plant morphogenesis. *Plant Cell* 12: 2129–2142.

Winey, M. and Culbertson, M.R. (1988) Mutations affecting the tRNA-splicing endonuclease activity of *Saccharomyces cerevisiae*. *Genetics* 118: 609–617.

Yao, Y., Ling, Q., Wang, H. and Huang, H. (2008) Ribosomal proteins promote leaf adaxial identity. *Development* 135: 1325–1334.